First-principles relativistic theory of the magnetic response of paramagnetic metals: Application to yttrium and scandium

V. Thakor,[1] J. B. Staunton,[1] J. Poulter,[2] S. Ostanin,[1] B. Ginatempo,[3] and Ezio Bruno[3]
[1]*Department of Physics, University of Warwick, Coventry CV4 7AL, United Kingdom*
[2]*Department of Mathematics, Faculty of Science, Mahidol University, Bangkok 10400, Thailand*
[3]*Dipartimento di Fisica and Unita INFM, Universita di Messina, Italy*
(Received 8 July 2003; published 7 October 2003)

We describe a first-principles theoretical formalism for the magnetic response of paramagnetic metals in which all relativistic effects such as spin-orbit coupling are included. In particular, the *easy axis* and dependence upon wave vector $\mathbf{q}$ of the paramagnetic spin susceptibility $\chi(\mathbf{q})$ can be calculated. To illustrate we apply the method to two transition metals, yttrium and scandium. In each case we find $\chi(\mathbf{q})$ to peak at a wave vector $\mathbf{q}=(0,0,0.57)\pi/c$, coincident with a Fermi surface nesting vector, and to have an easy axis perpendicular to $\mathbf{q}$. Since $\chi(\mathbf{q})$ plays a key role in determining the interaction between magnetic impurities in these metals, these results are consistent with the *helical* antiferromagnetic order found in many dilute rare-earth Y alloys. Conversely, the easy axis for the response to a uniform magnetic field, $\mathbf{q}=0$, lies along the c axis.

DOI: 10.1103/PhysRevB.68.134412 PACS number(s): 75.40.Cx, 71.15.Rf, 71.20.Be, 71.20.Eh

I. INTRODUCTION

A useful tool for studying metallic magnetism is the paramagnetic spin susceptibility, $\chi(\mathbf{q})$. It determines the response of a paramagnetic metal to a magnetic perturbation. For materials which order magnetically at low temperatures, a study of $\chi(\mathbf{q})$ for their higher temperature paramagnetic phases indicates the type of magnetic order to be found below the magnetic transition temperatures. The precursor spin fluctuations are described. If the greatest value of $\chi(\mathbf{q})$ is at $\mathbf{q}=(0,0,0)$, as in α-Fe, for example, ferromagnetic order is expected below the Curie temperature.[1] A peak for $\chi(\mathbf{Q})$ at some finite $\mathbf{q}=\mathbf{Q}$, on the other hand, signifies a more complicated antiferromagnetic (AF) structure with a modulation wave vector equal to $\mathbf{Q}$ as found in, say, Cr.[2] For metals which do not possess magnetic order at any temperature, $\chi(\mathbf{q})$ shows how the system reacts when doped by small concentrations of magnetic impurities.

If relativistic effects upon the motion of the itinerant electrons are neglected, the paramagnetic spin susceptibility is independent of the orientation of the applied magnetic field with respect to any crystalline axis of the material. Once, however, relativistic effects are included, the spin and orbital motion of the electrons are coupled and the spin rotational symmetry is broken, giving a preferred direction or *easy axis* to the magnetic response of the system. An example of a phenomenon which may be explained by a quantitative description of this effect is the relatively large anisotropic paramagnetostriction observed in some nearly magnetic metals.[3] When a magnetic field is applied to a cubic paramagnet such as Pd, PdRh, a strain is set up. The volume component can be explained quite straightforwardly in terms of the volume dependence of the spin susceptibility obtained from a nonrelativistic theory. The anisotropic (shape) paramagnetostriction, however, requires spin-orbit coupling effects to be included.[3]

In this paper we describe a ''first-principles'' theoretical formalism for the magnetic response of paramagnetic metals in which all relativistic effects such as spin-orbit coupling are considered. We show that the *easy axis* and its dependence upon wave vector $\mathbf{q}$ for the magnetic response can be calculated. We present specific calculations of the magnetic response of the transition metals yttrium and scandium. These case studies provide useful preparation for investigation of the magnetic response of the conduction electrons of rare-earth materials. Here the indirect exchange interactions which connect the localized $4f$ magnetic moments are typically described as Ruderman-Kittel-Kasuya-Yosida (RKKY) like and depend upon $\chi(\mathbf{q})$ of the conduction electrons.[4]

Although yttrium and scandium are not lanthanides, they do have several aspects in common with the heavier rare-earth (RE) metals. Both Y and Sc have similar hexagonal close packed (hcp) crystal structures and electronic configurations apart from the f electrons [i.e., $3d^14s^2$ (Sc), $4d^15s^2$ (Y), and $4f^75d^16s^2$ (Gd)] to the rare-earth elements. They also have similar electronic band structures near the Fermi energy.[5] Consequently, the topology of the Fermi surfaces of Y and Sc is similar to those of the RE's.[5] The salient feature is the *webbing* that contains flat parallel sheets perpendicular to the c axis leading to a strong Fermi nesting effect.[6] High quality samples of yttrium are more easily come by than the heavy rare earths and recent experiments[8] have measured directly the ''webbing'' feature of its Fermi surface. This strong Fermi nesting is thought to drive the helical antiferromagnetic ordering that many RE metals (i.e., Tb, Dy, Ho, Er) display, whereby the moments typically align in the basal plane and rotate their orientations in successive planes around the c axis. The anisotropic crystal field of the heavier lanthanides acts on the $4f$ electrons, which in turn determines the orientation of the local moments. The lack of magnetic moments (no f electrons) excludes magnetic ordering in pure Y and Sc. However, when Y is alloyed with very small amounts of magnetic impurities as low as $\sim 0.5\%$,[7,9,10] the result is helical antiferromagnetism with nesting vector close to that of Y.

The outline of this paper is as follows. In the next section

we describe our theory for the paramagnetic spin susceptibility in which relativistic effects are included. Following some calculational details we then discuss our study of the wave-vector dependence and easy axis of the magnetic response of both yttrium and scandium. The relation to the topology of the Fermi surfaces is shown. Since our formalism includes the effects of the Fermi-Dirac distribution on the effective single-electron energies, the calculated susceptibilities have a temperature dependence which we also show. In the final section we draw some conclusions and indicate what might be expected from future studies of rare-earth materials using this formalism.

II. RELATIVISTIC, PARAMAGNETIC, SPIN SUSCEPTIBILITY

We begin by considering a paramagnetic metal subjected to a small, external, inhomogeneous magnetic field, $\delta\mathbf{b}^{ext}(\mathbf{r})$, and obtain an expression for the induced magnetization $\delta\mathbf{m}(\mathbf{r})$. We use relativistic density-functional theory (RDFT) (Ref. 11) for finite temperatures[12] to treat the interacting electrons of the system and derive an expression via a variational linear-response approach.[13–15] Although there are a number of nonrelativistic studies of this type[16] here we include relativistic effects and pay particular attention to the magnetic anisotropy of the response. From our RDFT starting point we make a Gordon decomposition of the current density[11] and retain the spin-only part of the current, namely the spin magnetization $\mathbf{m}(\mathbf{r})$. This results in a *spin-only* version of RDFT,[11] in which the self-consistent solution of Kohn-Sham-Dirac equations is sought, i.e.,

$$[c\tilde{\boldsymbol{\alpha}}\cdot\hat{\mathbf{p}}+\tilde{\beta}mc^2+\tilde{\mathbf{1}}V^{eff}[\rho,\mathbf{m}]-\tilde{\beta}\tilde{\boldsymbol{\sigma}}\cdot\mathbf{b}^{eff}[\rho,\mathbf{m}]-\varepsilon]\times G(\mathbf{r},\mathbf{r}';\varepsilon)=\tilde{\mathbf{1}}\delta(\mathbf{r}-\mathbf{r}') \quad (1)$$

which describes the motion of a single electron through effective fields and $\tilde{\boldsymbol{\alpha}}$ and $\tilde{\beta}$ are Dirac 4×4 matrices. $G(\mathbf{r},\mathbf{r}';\varepsilon)$ is the one-electron Green's function and the charge $\rho(\mathbf{r})$ and magnetization densities $\mathbf{m}(\mathbf{r})$ can be written in terms of it, i.e.,

$$\rho(\mathbf{r})=-\mathrm{Tr}\int d\varepsilon f(\varepsilon,\mu,T)\frac{\mathrm{Im}}{\pi}G(\mathbf{r},\mathbf{r};\varepsilon),$$

$$\mathbf{m}(\mathbf{r})=-\mathrm{Tr}\,\tilde{\beta}\tilde{\boldsymbol{\sigma}}\int d\varepsilon f(\varepsilon,\mu,T)\frac{\mathrm{Im}}{\pi}G(\mathbf{r},\mathbf{r};\varepsilon), \quad (2)$$

where μ is the chemical potential, T the temperature, and $f(\varepsilon,\mu,T)$ the Fermi-Dirac function. These expressions are equivalent to sums over Fermionic Matsubara frequencies $\omega_n=i(2n+1)\pi k_BT$.[17] This equivalence can be exploited in the design of computational schemes for calculating such temperature-dependent quantities. The effective potential $V^{eff}[\rho,\mathbf{m}]$ consists of the usual combination of external potential (from the lattice of nuclei), the Hartree potential, and functional derivative of exchange-correlation energy $E_{xc}[\rho,\mathbf{m}]$ with respect to ρ while the effective magnetic field $\mathbf{b}^{eff}[\rho,\mathbf{m}]$ is the sum of any external magnetic field (from magnetic impurities, for example) and the functional derivative of E_{xc} with respect to magnetization. We use the local-density approximation (LDA) (Ref. 18) for E_{xc}. The leading relativistic effects contained in the Kohn-Sham-Dirac Hamiltonian of Eq. (1) are the well-known mass-velocity, Darwin, and spin-orbit coupling effects.

If a small external field $\delta\mathbf{b}^{ext}$ is applied along a direction $\hat{\mathbf{n}}$ with respect to the crystal axes of a paramagnetic system, a small magnetization $\delta\mathbf{m}(\mathbf{r})$ and effective magnetic field $\delta\mathbf{b}^{eff}$ are set up. The effective magnetic field is given by $\delta\mathbf{b}^{eff}[\rho(\mathbf{r}),\mathbf{m}(\mathbf{r})]=\delta\mathbf{b}^{ext}(\mathbf{r})+I_{xc}(\mathbf{r})\delta\mathbf{m}(\mathbf{r})$ where $I_{xc}(\mathbf{r})$ is the functional derivative of the effective exchange and correlation magnetic field (within the LDA) with respect to the induced magnetization density. The Green's function satisfying Eq. (1) can be expanded in a Dyson equation in terms of the unperturbed Green's function, $G_o(\mathbf{r},\mathbf{r}';\varepsilon)$ of the paramagnetic system ($\delta\mathbf{b}^{eff}=0$) and perturbation $\tilde{\beta}\tilde{\boldsymbol{\sigma}}.\delta\mathbf{b}^{eff}$ and the first-order terms enable the magnetic response function to be obtained.

For a general crystal lattice with N_s atoms located at positions $\mathbf{a}_l(l=1,\ldots,N_s)$ in each unit cell, a lattice Fourier transform can be carried out over lattice vectors $\{\mathbf{R}_i\}$. This can be written

$$\chi^{\hat{\mathbf{n}}}(\mathbf{x}_l,\mathbf{x}'_{l'},\mathbf{q})=\chi_o^{\hat{\mathbf{n}}}(\mathbf{x}_l,\mathbf{x}'_{l'},\mathbf{q})+\sum_{l''}^{N_s}\int\chi_o^{\hat{\mathbf{n}}}(\mathbf{x}_l,\mathbf{x}''_{l''},\mathbf{q})\times I_{xc}(\mathbf{x}''_{l''})\chi^{\hat{\mathbf{n}}}(\mathbf{x}''_{l''},\mathbf{x}'_{l'},\mathbf{q})d\mathbf{x}''_{l''}, \quad (3)$$

where the $\mathbf{x}_l$ are measured relative to the positions of atoms centered on $\mathbf{a}_l$. The noninteracting susceptibility of the static unperturbed system is given by

$$\chi_o^{\hat{\mathbf{n}}}(\mathbf{x}_l,\mathbf{x}'_{l'},\mathbf{q})=-(k_BT)\mathrm{Tr}\,\tilde{\beta}\tilde{\boldsymbol{\sigma}}\cdot\hat{\mathbf{n}}\sum_n\int\frac{d\mathbf{k}}{\nu_{BZ}}G_o(\mathbf{x}_l,\mathbf{x}'_{l'},\mathbf{k},\mu+i\omega_n)\tilde{\beta}\tilde{\boldsymbol{\sigma}}\cdot\hat{\mathbf{n}}G_o(\mathbf{x}'_{l'},\mathbf{x}_l,\mathbf{k}+\mathbf{q},\mu+i\omega_n). \quad (4)$$

The integral is over the Brillouin zone with wave vectors $\mathbf{k}$, $\mathbf{q}$, and $\mathbf{k}+\mathbf{q}$ within the Brillouin zone of volume ν_{BZ}. The sum is over the Fermionic Matsubara frequencies. The Green's function for the unperturbed, paramagnetic system containing the band-structure effects is obtained via relativistic multiple-scattering [Korringa-Kohn-Rostoker (KKR)] theory.[19] We solve Eq. (3) using a direct method of matrix inversion. The full Fourier transform is then generated

$$\chi^{\hat{\mathbf{n}}}(\mathbf{q})=(1/V)\sum_l\sum_{l'}e^{i\mathbf{q}\cdot(\mathbf{a}_l-\mathbf{a}'_{l'})}\times\int d\mathbf{x}_l\int d\mathbf{x}'_{l'}e^{i\mathbf{q}\cdot(\mathbf{x}_l-\mathbf{x}'_{l'})}\chi^{\hat{\mathbf{n}}}(\mathbf{x}_l,\mathbf{x}'_{l'},\mathbf{q}), \quad (5)$$

where V is the volume of the unit cell. Some aspects of the numerical methods used to evaluate Eqs. (3)–(5) of this type can be found in Refs. 15 and 20. Note that this expression for the noninteracting susceptibility can be shown to be formally equivalent to one of the familiar type

$$\chi_o^{\hat{\mathbf{n}}}(\mathbf{q}) \propto \int d\mathbf{k} \sum_{j,j'} \frac{|M_{j,j'}(\mathbf{k},\mathbf{k}+\mathbf{q},\hat{\mathbf{n}})|^2 f_{\mathbf{k},j}(1-f_{\mathbf{k}+\mathbf{q},j'})}{\varepsilon_{j'}^{\hat{\mathbf{n}}}(\mathbf{k}+\mathbf{q}) - \varepsilon_j^{\hat{\mathbf{n}}}(\mathbf{k})}, \tag{6}$$

where j and j' are electronic-band indices, $\varepsilon_j^{\hat{\mathbf{n}}}(\mathbf{k})$ a single-electron energy, M is a matrix element, and $f_{\mathbf{k},j} = f(\varepsilon_j^{\hat{\mathbf{n}}}(\mathbf{k}),\mu,T)$, the Fermi-Dirac function.

The important feature of the response function [Eqs. (3)–(5)], is its dependence on the direction of the magnetic field $\hat{\mathbf{n}}$. This vanishes for the nonrelativistic version of the formalism since it is caused by spin-orbit coupling. A measure of this anisotropy is given as the difference in the noninteracting susceptibility when an external magnetic field is applied in two directions with respect to the crystal axes, i.e., $(\chi_o^{\hat{\mathbf{n}}_1} - \chi_o^{\hat{\mathbf{n}}_2})$. The anisotropy of the full susceptibility $(\chi^{\hat{\mathbf{n}}_1} - \chi^{\hat{\mathbf{n}}_2})$ can be calculated from Eq. (3). The approach presented here is applicable to ordered compounds and elemental metals and can be modified to study disordered alloys[15] owing to its KKR multiple-scattering framework. In the next section we describe calculations of the magnetic response of the $4d$ hcp metal yttrium and in order to gauge the importance of these relativistic effects with atomic number, we compare our calculations with those for Y's lighter $3d$ counterpart Sc.

III. WAVE-VECTOR DEPENDENCE AND EASY AXIS OF THE MAGNETIC RESPONSE OF YTTRIUM AND SCANDIUM

We use atomic sphere approximation (ASA), effective one-electron potentials and charge densities in the calculations for Y and Sc with experimental lattice constants $a = 6.89$, $c = 10.83$ and $a = 6.24$, $c = 9.91$, respectively, in atomic units a_0.[21] The details of the electronic structures using a fully relativistic KKR method compare well with those from full-potential calculations.[22] The Fermi surface for Y in the H-L-M-K plane is shown in Fig. 1(a). It shows two relatively flat parallel sheets. The nesting vector $\mathbf{q}_{inc} = \pi/c(0,0,0.57)$ is indicated by the arrow. Figure 1(a) is in very good agreement with previous calculations[6] and experiments.[8,23] Dugdale *et al.*[8] have recently carried out positron annihilation Fermiology experiments and measured $\mathbf{q}_{inc} = \pi/c(0,0,0.55 \pm 0.02)$ for Y. Also, Vinokurova *et al.*[23] measured $\mathbf{q}_{inc} \approx \pi/c(0,0,0.58)$. We find a similar Fermi surface for Sc with the same nesting vector $\mathbf{q}_{inc} = \pi/c(0,0,0.57)$, also in good agreement with earlier calculations.[24]

Our calculations of the enhanced static susceptibility, defined by Eq. (3), show a peak at this same wave vector $\mathbf{q}_{inc} = \pi/c(0,0,0.57)$ for both Y and Sc. This is shown in Fig. 1(b), where we probe wave vectors along the c axis from Γ to A. [The special point A for hcp crystal structures is $(0,0,\pi/c)$.] Results are shown for a temperature of 100 K for these calculations.

In terms of polar and azimuth angles θ,φ the direction is written $\hat{\mathbf{n}} = (\sin\theta\cos\varphi, \sin\theta\sin\varphi, \cos\theta)$. For hcp systems such as Y or Sc, if an external magnetic field is applied along the $\hat{\mathbf{n}} = (0,0,1)$ direction, i.e., the c axis, where $(\theta,\varphi) \rightarrow (0,0)$, χ_o^z is produced. On the other hand, χ_o^x is the response of the system when the field is applied in the ab plane, $\hat{\mathbf{n}} = (1,0,0)$ and $(\theta,\varphi) \rightarrow (\pi/2,0)$. Figure 2(a) shows the anisotropy $\chi_o^{\hat{\mathbf{n}}}(\mathbf{q},\theta,\varphi) - \chi_o^z(\mathbf{q})$ as a function of θ for Y and Sc at $\mathbf{q}_{inc}$ and $\mathbf{q}_o \simeq (0,0,0)$. We find the anisotropy of this linear-response function to be invariant in φ so that the magnetic response is insensitive to the direction along which an external magnetic field is applied in the ab plane. As θ is increased, an anisotropy is observed which reaches a maximum at $\theta = \pi/2$ as shown in Fig. 2(a). In fact, we observe that the anisotropy takes the rather simple form

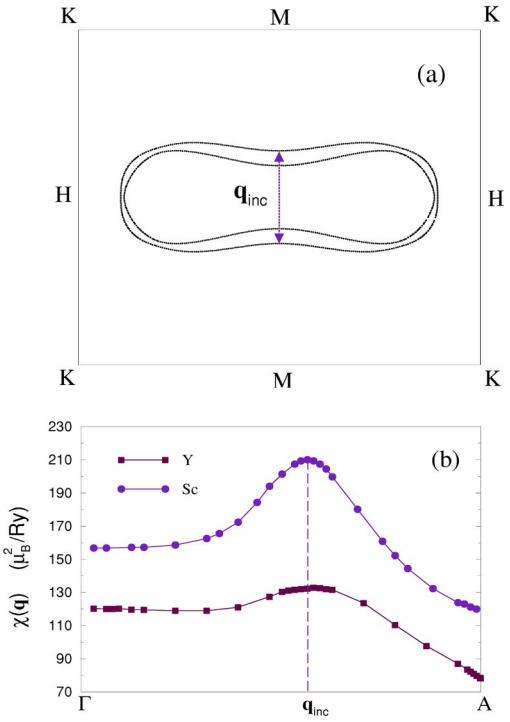

FIG. 1. (a) Cross section of the webbing Fermi surface in the H-L-M-K plane for Y. The nesting vector is indicated by the arrow. The special point L lies at the center. (b) The enhanced susceptibility for Y and Sc along the Γ-A direction for $T = 100$ K. For wave vectors $\mathbf{q}$ close to A the gradient of the function diminishes and is zero at A.

$$\chi_o^{\hat{\mathbf{n}}}(\mathbf{q},\theta,\varphi) - \chi_o^z(\mathbf{q}) = [\chi_o^x(\mathbf{q}) - \chi_o^z(\mathbf{q})] \cdot |\hat{\mathbf{q}} \times \hat{\mathbf{n}}|^2 \tag{7}$$

for hcp crystal structures[25] ($|\hat{\mathbf{q}} \times \hat{\mathbf{n}}| = \sin\theta$). It is therefore sufficient to show $\chi_o^x(\mathbf{q}) - \chi_o^z(\mathbf{q})$, to determine the easy axes of the magnetic response. Figure 2(b) shows the weak temperature dependence of the anisotropy of Y and Sc at both the nesting vector $\mathbf{q}_{inc}$ and also at $\mathbf{q}_o \simeq (0,0,0)$. As expected, the anisotropy is an order of magnitude larger for Y than for Sc. This difference is a result of spin-orbit coupling being more pronounced in the heavier $4d$ metal Y than in the $3d$ Sc. We infer that a still greater but similar anisotropy should be evident in the magnetic response of the $5d$ conduction electrons in the heavier still RE materials.

IV. CONCLUSION

It is apparent from Figs. 1 and 2 that Y shows its strongest response at the wave vector $\mathbf{q}_{inc}$ which corresponds to the

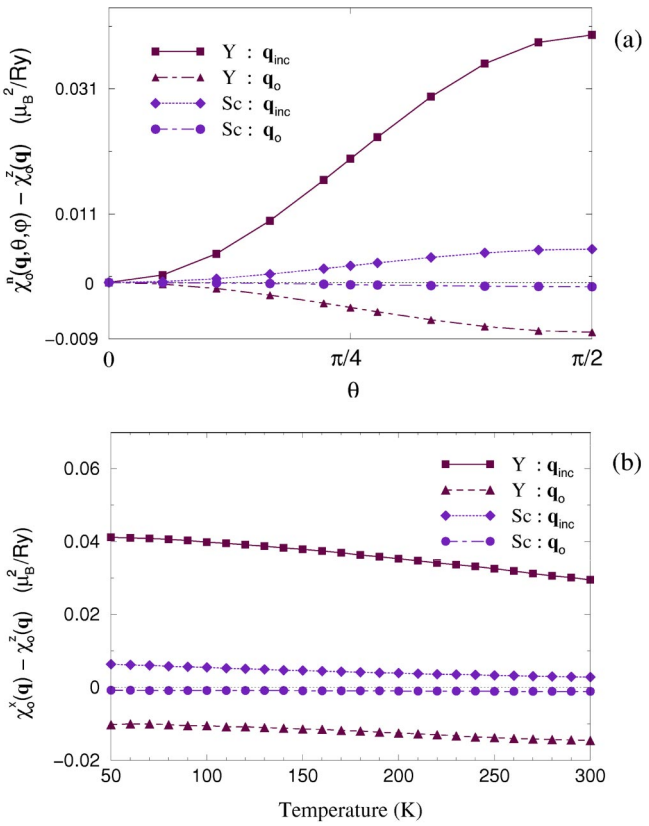

FIG. 2. (a) The anisotropy as a function of θ for Y and Sc at $\mathbf{q}_{inc}=\pi/c(0,0,0.57)$ and $\mathbf{q}_o \simeq (0,0,0)$ and at $T=100$ K. (b) The temperature dependence of the anisotropy of Y and Sc at both the nesting vector $\mathbf{q}_{inc}$ and $\mathbf{q}_o$.

Fermi Surface (FS) nesting and that the response here is strongest to magnetic fields directed in the basal *ab* plane. This is consistent with onset of long-range helical antiferromagnetic ordering found in very dilute rare-earth yttrium alloys such as Tb-Y, Dy-Y, and Ho-Y.[7] A simple description can be given in terms of the indirect Ruderman-Kittel-Kasuya-Yosida (RKKY) exchange interaction.[4] Here the localized $4f$ moments of the RE impurities interact via the conduction electrons of yttrium whose magnetic properties are described by the spin susceptibility $\chi(\mathbf{q})$. Since $\chi(\mathbf{q_{inc}})$ has an easy axis perpendicular to $\mathbf{q_{inc}}$ a helical incommensurate antiferromagnetic structure is favored for the magnetic impurities.

Potential future applications of this magnetic response formalism include studies of more concentrated RE-Y alloys and also the RE elements themselves. The $4f$ electrons would need to be considered explicitly and $\chi(\mathbf{q})$ used to describe their coupling to the conduction electrons. The Gd-Y alloy system presents an interesting range of behavior. Pure gadolinium has a ferromagnetic phase with the easy axis along the *c* axis so that in the paramagnetic phase at higher temperatures $\chi(\mathbf{q})$ should peak at $\mathbf{q}=(0,0,0)$. Moreover, its FS has been observed not to possess a webbing feature.[26] Some recent experiments[26] have shown that adding more than around 30% Y to Gd changes the topology of the Fermi surface of the paramagnetic phase and the webbing is observed again. This is coincident with the alloys' forming helical AF states at lower temperatures. Calculations of $\chi(\mathbf{q})$ above the Néel temperature should then peak at this nesting vector. Moreover, in this concentration range, neutron diffraction[10,26] has shown that application of a modest uniform magnetic field along the *c* axis can lead to a ferromagnetic alignment of the Gd moments along the *c* axis. Once the magnetic field is switched off the system reverts to its helical AF state. This suggests that the alloys' $\chi(\mathbf{q})$'s and anisotropies are similar to those shown in Figs. 1(b) and 2(a) but with the relative peak heights of $\chi(\mathbf{q})$ at $\mathbf{q}=(0,0,0)$ and $\mathbf{q}_{inc}$ to be finely balanced.

In summary, we have described an *ab initio* theoretical formalism to calculate the relativistic static paramagnetic spin susceptibility for metals at finite temperatures. Since relativistic effects such as spin-orbit coupling are included we can identify the anisotropy or *easy axes* of the magnetic response. We applied this formalism to the $4d$ metal Y and for comparison with the lighter $3d$ Sc. The enhanced susceptibility for both these metals displays a peak at the incommensurate wave vector $\mathbf{q}_{inc}=(0,0,0.57\pi/c)$, traceable to a FS nesting feature found in the calculated electronic structure and Fermiology experiments.[8,23] The anisotropy results for both Y and Sc indicate that the easy axis at $\mathbf{q}_{inc}$ lies in the basal plane, while for $\mathbf{q}=(0,0,0)$ is parallel to the crystal *c* axis.

ACKNOWLEDGMENT

The authors acknowledge support from EPSRC (UK).

[1] J. B. Staunton, Rep. Prog. Phys. **57**, 1289 (1994).
[2] E. Fawcett, Rev. Mod. Phys. **60**, 209 (1988).
[3] E. Fawcett and V. Pluzhnikov, Physica B & C **119B**, 161 (1983); P. G. Averbuch and P. J. Segransan, Phys. Rev. B **4**, 2067 (1971).
[4] T. Kasuya, in *Magnetism*, edited by G. T. Rado and H. Suhl (Academic Press Inc., New York, 1966), Vol. IIB, p. 215.
[5] S. C. Keeton and T. L. Loucks, Phys. Rev. **168**, 672 (1968).
[6] T. L. Loucks, Phys. Rev. **144**, 504 (1966).
[7] H. R. Child, W. C. Koehler, E. O. Wollan, and J. W. Cable, Phys. Rev. **138**, A1655 (1965); R. Caudron, H. Bouchiat, P. Monod, P. J. Brown, R. Chung, and J. L. Tholence, Phys. Rev. B **42**, 2325 (1990).
[8] S. B. Dugdale, H. M. Fretwell, M. A. Alam, G. Kontrym-Sznajd, R. N. West, and S. Badrzadeh, Phys. Rev. Lett. **79**, 941 (1997).
[9] N. Wakabayashi and R. M. Nicklow, Phys. Rev. B **10**, 2049 (1974); P. J. Brown, R. Caudron, A. Fert, D. Givord, and P. Pureur, J. Phys. (France) Lett. **46**, L1139 (1985); L. E. Wenger, J. W. Hunter, J. A. Mydosh, J. A. Gotaas, and J. J. Rhyne, Phys. Rev. Lett. **56**, 1090 (1986).
[10] S. Bates, S. B. Palmer, J. B. Sousa, G. J. McIntyre, D. Fort, S.

Legvold, B. J. Beaudry, and W. C. Koehler, Phys. Rev. Lett. **55**, 2425 (1985).
[11] A. K. Rajagopal and J. Callaway, Phys. Rev. B **7**, 1912 (1973); A. H. MacDonald and S. H. Vosko, J. Phys. C **12**, 2977 (1979).
[12] N. D. Mermin, Phys. Rev. **137**, A1441 (1965).
[13] S. H. Vosko and J. P. Perdew, Can. J. Phys. **53**, 1385 (1975).
[14] A. H. MacDonald and S. H. Vosko, J. Low Temp. Phys. **25**, 27 (1976); M. Matsumoto, J. B. Staunton, and P. Strange, J. Phys.: Condens. Matter **2**, 8365 (1990).
[15] J.B. Staunton, J. Poulter, B. Ginatempo, E. Bruno, and D. D. Johnson, Phys. Rev. Lett. **82**, 3340 (1999); J. B. Staunton, J. Poulter, B. Ginatempo, E. Bruno, and D. D. Johnson, Phys. Rev. B **62**, 1075 (2000).
[16] E. Stenzel and H. Winter, J. Phys. F **16**, 1789 (1986); S. Y. Savrasov, Phys. Rev. Lett. **81**, 2570 (1998).
[17] A. L. Fetter and J. D. Walecka, *Quantum Theory of Many Particle Systems* (McGraw-Hill, New York, 1971).
[18] U. von Barth and L. Hedin, J. Phys. C **5**, 1629 (1972).
[19] J. S. Faulkner and G. M. Stocks, Phys. Rev. B **21**, 3222 (1980); P. Strange, H. Ebert, J. B. Staunton, and B. L. Gyorffy, J. Phys.: Condens. Matter **1**, 2959 (1989).
[20] V. Thakor, Ph.D. thesis, University of Warwick, 2003.
[21] *Pearson's Handbook of Crystallographic Data for Intermetallic Phases* (American Society for Metals, Metals Park, OH, 1985).
[22] K. Schwarz, P. Blaha, and G. K. H. Madsen, Comput. Phys. Commun. **147**, 71 (2002).
[23] L. I. Vinokurova, A. G. Gapotchenko, E. S. Itskevich, E. T. Kulatov, and N. I. Kulikov, Pis'ma Zh. Eksp. Teor. Fiz. **34**, 590 (1981) [JETP Lett. **34**, 566 (1981)].
[24] G. S. Flemming and T. L. Loucks, Phys. Rev. **173**, 685 (1968).
[25] We also find this relationship to hold for tetragonal crystal structures.
[26] H. M. Fretwell, S. B. Dugdale, M. A. Alam, D. C. R. Hedley, A. Rodriguez-Gonzalez, and S. B. Palmer, Phys. Rev. Lett. **82**, 3867 (1999).